62 72285 Copy 576

CONFIDENTIAL

NASA TM X-461

NASA TM X-461

29 COPIES

# TECHNICAL MEMORANDUM

## X-461

# LONGITUDINAL AERODYNAMIC CHARACTERISTICS AT A MACH NUMBER OF 1.97 OF A SERIES OF RELATED WINGED REENTRY CONFIGURATIONS FOR ANGLES OF ATTACK FROM 0° TO 90°


By Gerald V. Foster

Langley Research Center
Langley Field, Va.


[redacted]

Declassified by authority of NASA
Classification Change Notices No. 113
Dated ** 2-14-68

[redacted]


NATIONAL AERONAUTICS AND SPACE ADMINISTRATION

WASHINGTON March 1961


[redacted]

1H

DECLASSIFIED

CONFIDENTIAL

NATIONAL AERONAUTICS AND SPACE ADMINISTRATION

TECHNICAL MEMORANDUM X-461

# LONGITUDINAL AERODYNAMIC CHARACTERISTICS AT A MACH NUMBER OF 1.97 OF A SERIES OF RELATED WINGED REENTRY CONFIGURATIONS FOR ANGLES OF ATTACK FROM 0° TO 90°*

By Gerald V. Foster

L-650

## SUMMARY

An investigation has been conducted to determine the longitudinal aerodynamic characteristics of a series of winged-body reentry configurations through an angle-of-attack range from 0° to 90° at a Mach number of 1.97. The configurations included a trapezoidal-wing series, a delta-wing series, a trailing-edge-sweep series, and a circular planform.

The results indicated that although all configurations tested were stable at angles of attack from about 60° to 90°, the stability varied nonlinearly with angle of attack with regions of instability occurring below an angle of attack of about 60°.

## INTRODUCTION

The reentry phase of a space vehicle is of particular importance since maximum heating and decelerating forces occur during this phase of flight. Obviously the reduction of these factors to human tolerances is a prime requisite for manned space vehicles. One approach being considered by the National Aeronautics and Space Administration consists of a winged vehicle which would reenter the atmosphere at an angle of attack approaching 90° and thereby provide a high-drag reentry while maintaining some lift for the trajectory control required to minimize heating. A discussion of some methods of controlling the trajectories of high-drag—low-lift vehicles entering the earth's atmosphere is presented in reference 1. References 2 and 3 present

---

*Title, Unclassified.

[redacted]

the longitudinal aerodynamic characteristics of some delta-wing configurations at subsonic and supersonic speeds. References 2 and 3 indicate that although the configurations were longitudinally stable at angles of attack approaching 90°, the pitching moment varied nonlinearly with angle of attack. As a result the control problem of such a vehicle would be complex.

Only a limited amount of aerodynamic information is available for reentry vehicles at angles of attack approaching 90°. Hence, an investigation of the longitudinal aerodynamic characteristics of a series L
of winged reentry configurations through a large angle-of-attack range 6
is being conducted by the NASA for speeds ranging from transonic to 5
hypersonic. 0

This paper presents the aerodynamic characteristics of ten winged reentry configurations tested at a Mach number of 1.97 in the Langley 4- by 4-foot supersonic pressure tunnel through an angle-of-attack range from 0° to 90°. The data are presented without analysis.

## SYMBOLS

The results obtained with the various models were reduced to coefficient form by utilizing the geometric characteristics of the respective models. The pitching moment, normal force, and axial force are referred to the body axis system, and the lift and drag coefficients are referred to the wind axis system. The moment coefficients of each model are referred to the point on the body center line which corresponds to the wing center of area (specified individually in table I).

$C_m$ pitching-moment coefficient, $\frac{\text{Pitching moment}}{qS\bar{c}}$

$C_N$ normal-force coefficient, $\frac{\text{Normal force}}{qS}$

$C_A$ axial-force coefficient, $\frac{\text{Axial force}}{qS}$

$C_L$ lift coefficient, $\frac{\text{Lift}}{qS}$

$C_D$ drag coefficient, $\frac{\text{Drag}}{qS}$

$q$ free-stream dynamic pressure

DECLASSIFIED



| | |
|---|---|
| $S$ | wing area |
| $\bar{c}$ | mean geometric chord |
| $L/D$ | lift-drag ratio |
| $M$ | Mach number |
| $\alpha$ | angle of attack, deg |
| $\Lambda_{LE}$ | leading-edge sweep angle, deg |
| $\Lambda_{TE}$ | trailing-edge sweep angle, deg |

## MODEL AND APPARATUS

Ten wing-body configurations differing primarily in wing planform were used in these tests. A typical arrangement of a wing and body used in this investigation is shown in figure 1. The wings were constructed of 1/4-inch-thick sheet metal and the planforms tested were trapezoidal, swept, delta, and circular. The geometric characteristics of all wing planforms investigated, except for the circular, are presented in figure 2, and of all wing planforms, in table I. Each of these wings had a planform area of approximately 0.4 square foot. The disk had a diameter of 8.56 inches and a mean geometric chord of 7.72 inches. The edge of the disk was finished perpendicular to the upper and lower surfaces; whereas, the leading edges of the other wing planforms were finished with a 1/8-inch radius. The body was composed of a straight section with an arbitrarily faired forebody. Because of the variation in wing root chords, adjustments were made in the forebody length so that the body extended from the trailing edge of the wing at the root chord to approximately the leading edge of the wing at the root chord.

The models were mounted in the tunnel on a support system which permitted variation of angle of attack from $0^{\circ}$ to $90^{\circ}$ (fig. 3). The force and moment characteristics were obtained through the use of an internal six-component strain-gage balance. In varying the angle of attack, the model was rotated about a point which coincided with the balance center.

## TESTS, CORRECTIONS, AND ACCURACY

The tests were made at a Mach number of 1.97, a stagnation temperature of 100° F, and a stagnation pressure of 6 pounds per square inch absolute. The stagnation dewpoint was maintained sufficiently low (-25° F or below) to prevent condensation effects from being encountered in the test section. The tests were made through an angle-of-attack range from 0° to 90° at a sideslip angle of 0°.

The angles of attack were corrected for deflection of the balance and sting under load. The model-support method used in these tests may introduce sting-interference effects at large angles of attack; however, no attempt was made to determine whether the models were affected by sting interference.

Estimated probable errors in the data based on repeatability, zero shifts, calibration, and random errors of instruments are as follows:

| | |
|---|---|
| $C_N$ . . . . . . . . . . . . . . . . . . . . . . . . . . . . . . | ±0.030 |
| $C_A$ . . . . . . . . . . . . . . . . . . . . . . . . . . . . . . | ±0.005 |
| $C_m\bar{c}$, in. . . . . . . . . . . . . . . . . . . . . . . . . . . | ±0.037 |
| $\alpha$, deg . . . . . . . . . . . . . . . . . . . . . . . . . . . | ±0.1 |
| M . . . . . . . . . . . . . . . . . . . . . . . . . . . . . . . | ±0.01 |

## PRESENTATION OF RESULTS

Aerodynamic characteristics of the trapezoidal-wing models, the delta-wing models, and the trailing-edge-sweep models are presented in figures 4, 5, and 6, respectively. The results for the disk-planform model are presented for comparison purposes in each figure.

## SUMMARY OF RESULTS

The results of an investigation of the longitudinal aerodynamic characteristics of a series of related winged reentry configurations indicate that although all configurations tested were stable at angles of attack from about 60° to 90°, the stability, in general, varied nonlinearly with angle of attack with regions of instability occurring below an angle of attack of approximately 60°. The large negative pitching moments at low angles of attack are the result of the asymmetrical body arrangement. The highly swept delta-wing configurations and the swept-forward trailing-edge configuration experienced the least change in stability with angle of attack.

The differences in axial-force level for the various configurations are caused by changes in forebody bluntness as the root chord length is varied. Thus, the values of lift-drag ratio are also affected by forebody bluntness.

Langley Research Center,
National Aeronautics and Space Administration,
Langley Field, Va., December 6, 1960.

L
6
5
0

## REFERENCES

1. Eggleston, John M., and Young, John W.: Trajectory Control for Vehicles Entering the Earth's Atmosphere at Small Flight-Path Angles. NASA TR R-89, 1961. (Supersedes NASA MEMO 1-19-59L.)

2. Spencer, Bernard, Jr.: High-Subsonic-Speed Investigation of the Static Longitudinal Aerodynamic Characteristics of Several Delta-Wing Configurations for Angles of Attack From 0° to 90°. NASA TM X-168, 1959.

3. Foster, Gerald V.: Exploratory Investigation at Mach Number of 2.01 of the Longitudinal Stability and Control Characteristics of a Winged Reentry Configuration. NASA TM X-178, 1959.

TABLE I.- GEOMETRIC CHARACTERISTICS OF MODELS

(a) Trapezoidal-wing series

| | |
|---|---|
| $55^{\circ}$ sweptback wing: | |
| Span, in. | 8.26 |
| Root chord, in. | 11.00 |
| Tip chord, in. | 3.30 |
| Area, sq ft | 0.409 |
| Mean geometric chord, in. | 7.85 |
| Aspect ratio | 1.15 |
| Center of area from wing apex, in. | 6.34 |
| Body length, in. | 10.65 |
| $59^{\circ}$ sweptback wing: | |
| Span, in. | 8.26 |
| Root chord, in. | 11.00 |
| Tip chord, in. | 3.30 |
| Area, sq ft | 0.409 |
| Mean geometric chord, in. | 7.85 |
| Aspect ratio | 1.15 |
| Center of area from wing apex, in. | 6.67 |
| Body length, in. | 10.65 |
| $63^{\circ}$ sweptback wing: | |
| Span, in. | 8.26 |
| Root chord, in. | 11.00 |
| Tip chord, in. | 3.30 |
| Area, sq ft | 0.409 |
| Mean geometric chord, in. | 7.85 |
| Aspect ratio | 1.15 |
| Center of area from wing apex, in. | 7.08 |
| Body length, in. | 10.65 |

(b) Delta-wing series

| | |
|---|---|
| $55^{\circ}$ sweptback wing: | |
| Span (actual), in. | 11.06 |
| Root chord, in. | 8.45 |
| Area, sq ft | 0.404 |
| Mean geometric chord, in. | 6.29 |
| Aspect ratio | 2.10 |
| Center of area from wing apex, in. | 5.36 |
| Body length, in. | 8.34 |
| $65^{\circ}$ sweptback wing: | |
| Span (actual), in. | 9.55 |
| Root chord, in. | 10.06 |
| Area, sq ft | 0.404 |
| Mean geometric chord, in. | 7.73 |
| Aspect ratio | 1.57 |
| Center of area from wing apex, in. | 6.28 |
| Body length, in. | 9.94 |
| $75^{\circ}$ sweptback wing: | |
| Span (actual), in. | 7.53 |
| Root chord, in. | 12.20 |
| Area, sq ft | 0.404 |
| Mean geometric chord, in. | 10.09 |
| Aspect ratio | 0.98 |
| Center of area from wing apex, in. | 7.43 |
| Body length, in. | 12.09 |

L-650

TABLE I.- GEOMETRIC CHARACTERISTICS OF MODELS - Concluded

(c) Wing trailing-edge-sweep series

| | |
|---|---|
| **Wing trailing edge swept back:** | |
| Span, in. | 9.14 |
| Root chord, in. | 8.57 |
| Tip chord (theoretical), in. | 3.00 |
| Area, sq ft | 0.404 |
| Mean geometric chord, in. | 7.33 |
| Aspect ratio | 1.44 |
| Center of area from wing apex, in. | 6.24 |
| Body length, in. | 8.34 |
| **Wing trailing edge swept 0°:** | |
| Span, in. | 7.86 |
| Root chord, in. | 10.32 |
| Tip chord (theoretical), in. | 3.39 |
| Area, sq ft | 0.404 |
| Mean geometric chord, in. | 8.27 |
| Aspect ratio | 1.07 |
| Center of area from wing apex, in. | 6.23 |
| Body length, in. | 9.94 |
| **Wing trailing edge swept forward:** | |
| Span, in. | 7.86 |
| Root chord, in. | 11.35 |
| Tip chord (theoretical), in. | 2.16 |
| Area, sq ft | 0.404 |
| Mean geometric chord | 8.84 |
| Aspect ratio | 1.07 |
| Center of area from wing apex, in. | 6.29 |
| Body length, in. | 9.94 |

(d) Disk

| | |
|---|---|
| Diameter, in. | 8.56 |
| Area, sq ft | 0.409 |
| Mean geometric chord, in. | 7.72 |
| Aspect ratio | 1.25 |
| Center of area from leading edge of wing at root chord, in. | 4.28 |
| Body length, in. | 8.34 |

CONFIDENTIAL

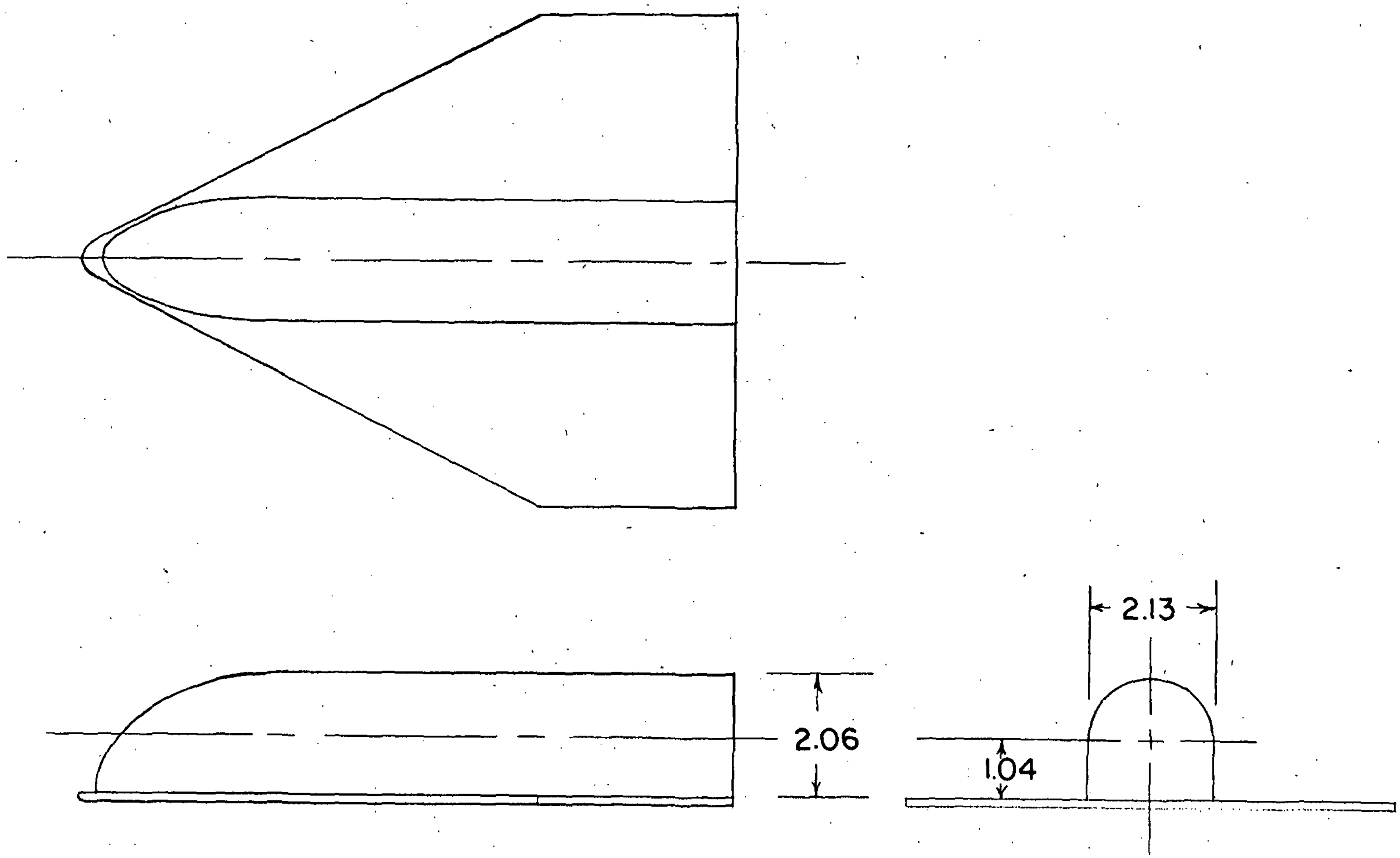


Figure 1.- Three-view drawing illustrating typical wing-body arrangement. All dimensions are in inches.

L-650

DECLASSIFIED



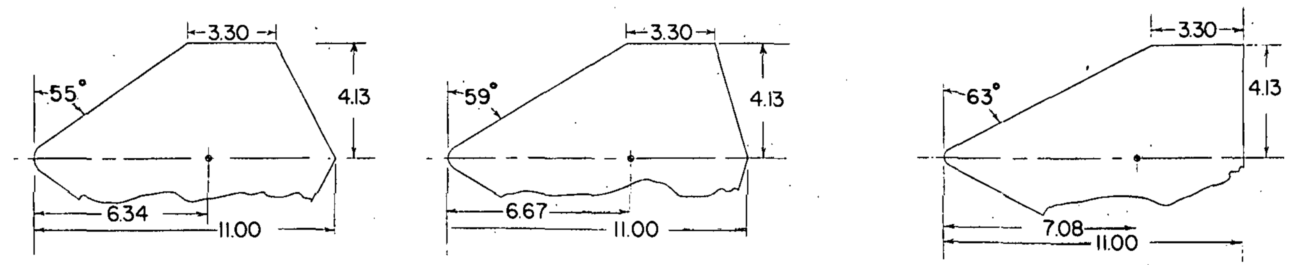


(a) Trapezoidal-wing series.

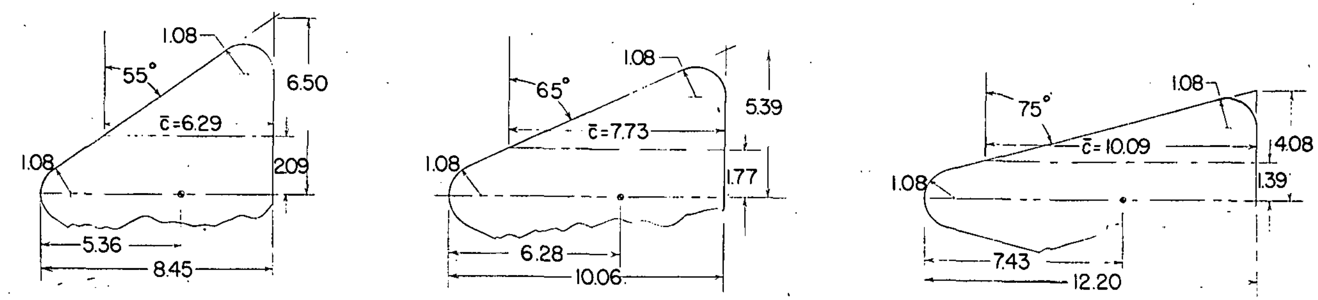


(b) Delta-wing series.

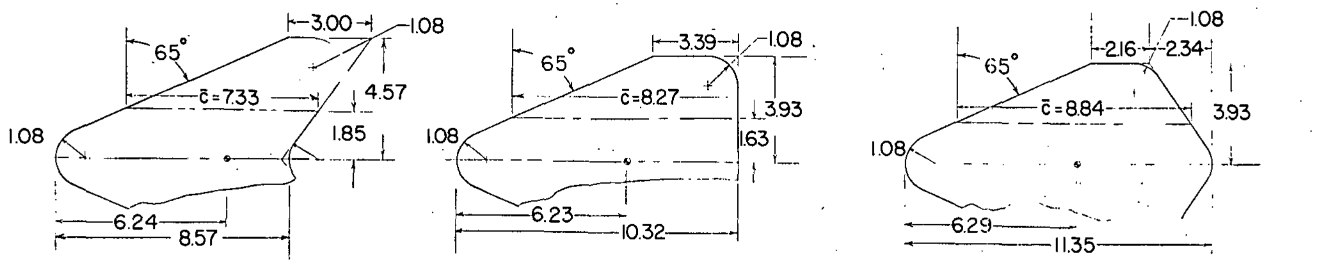


(c) Trailing-edge-sweep series.

Figure 2.- Details of models. All linear dimensions are in inches.

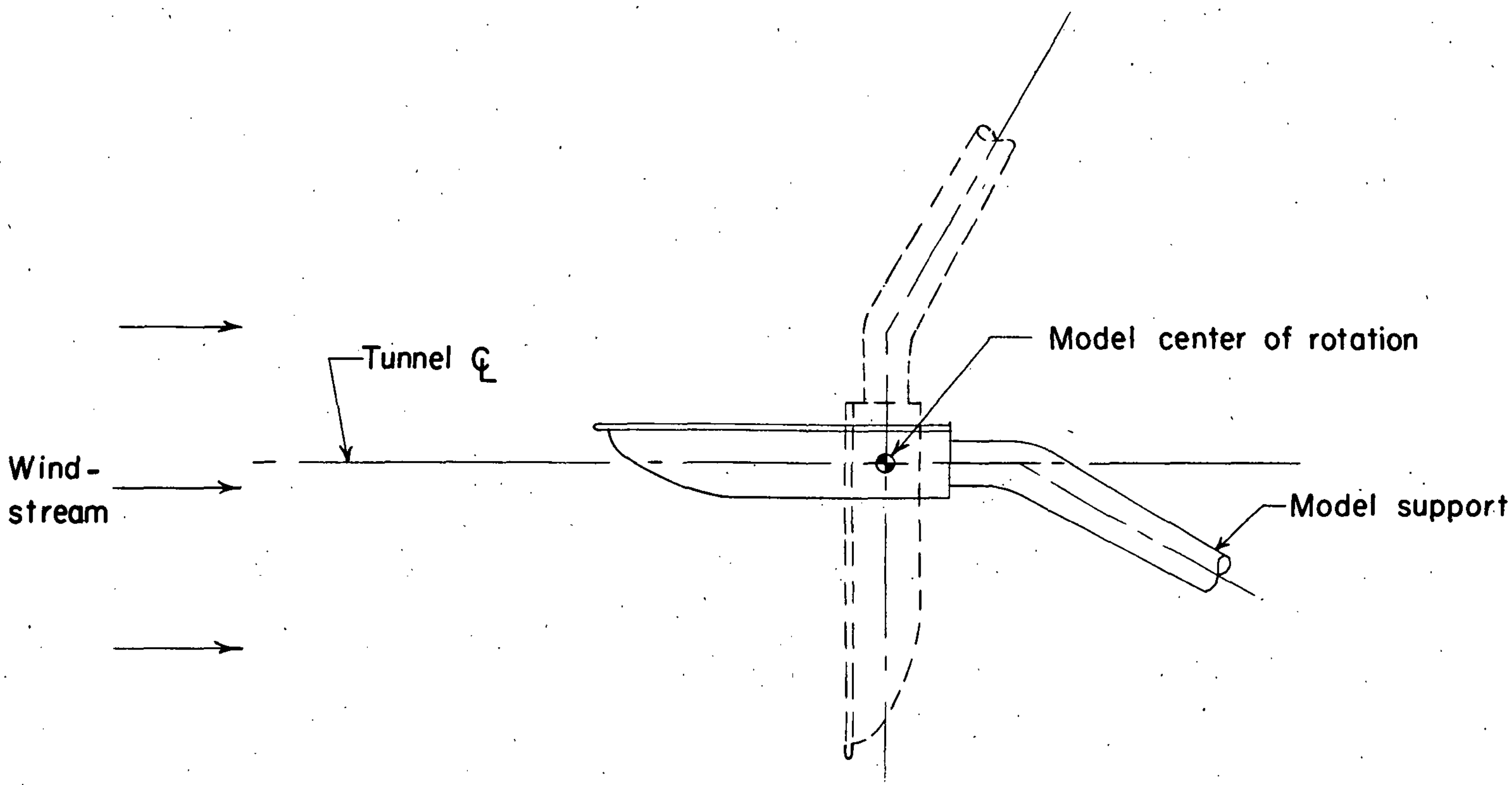


Figure 3.- Schematic diagram illustrating model test position at angles of attack of $0^{\circ}$ and $90^{\circ}$.

I-650

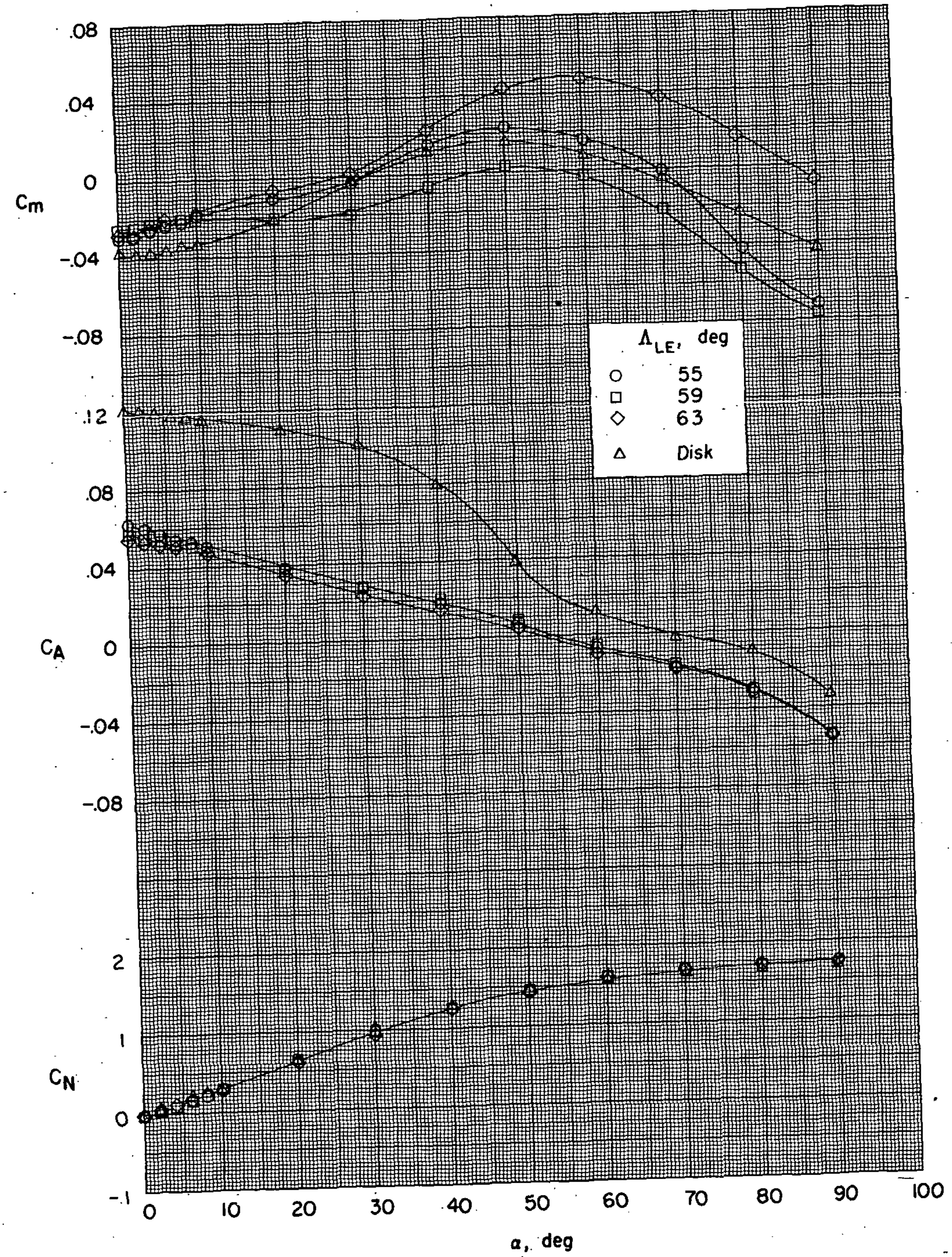


(a) $C_m$, $C_A$, and $C_N$.

Figure 4.- Aerodynamic characteristics of trapezoidal-wing models.

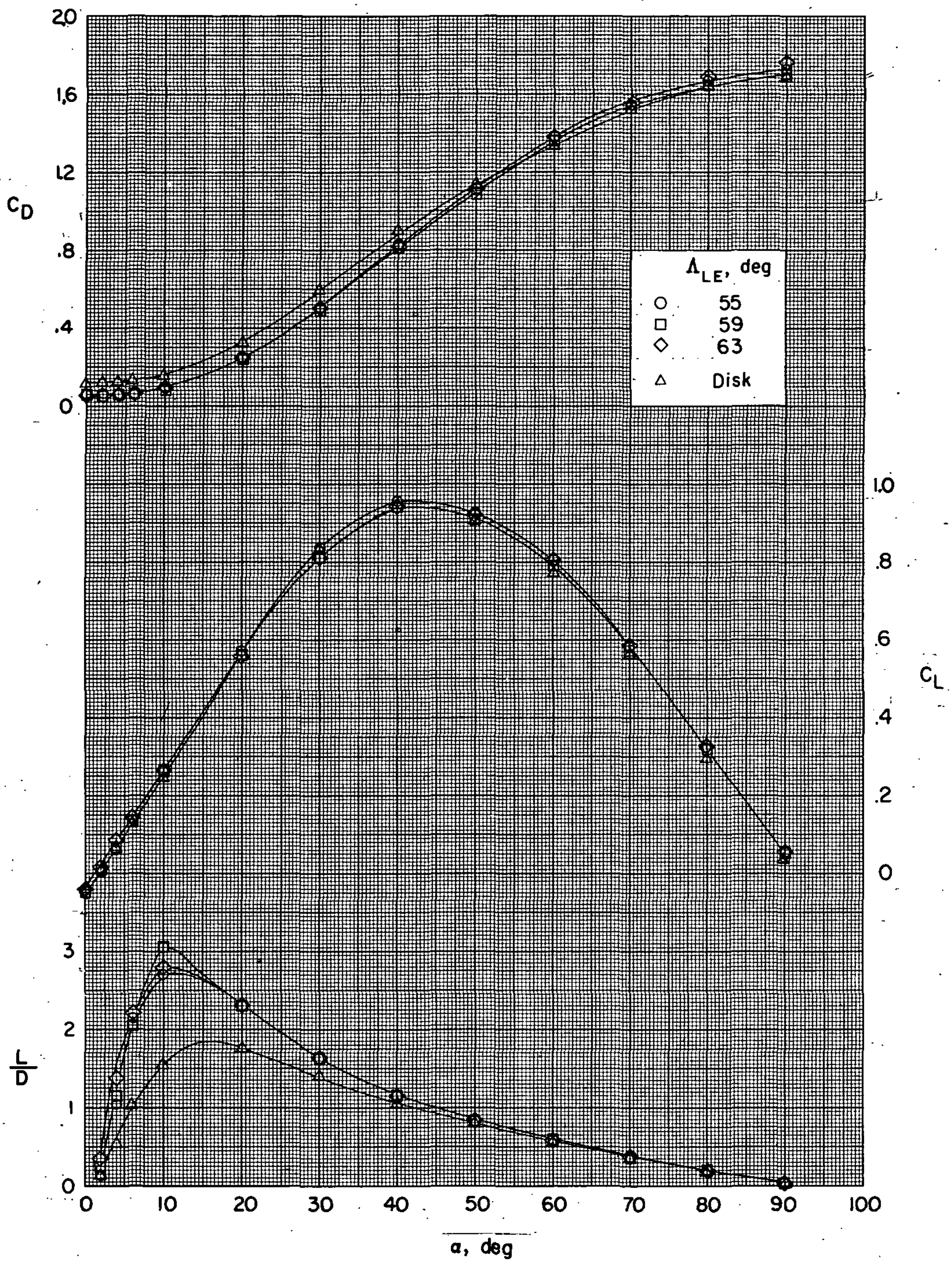


(b) $C_D$, $C_L$, and L/D.

Figure 4.- Concluded.

L-650

L-650

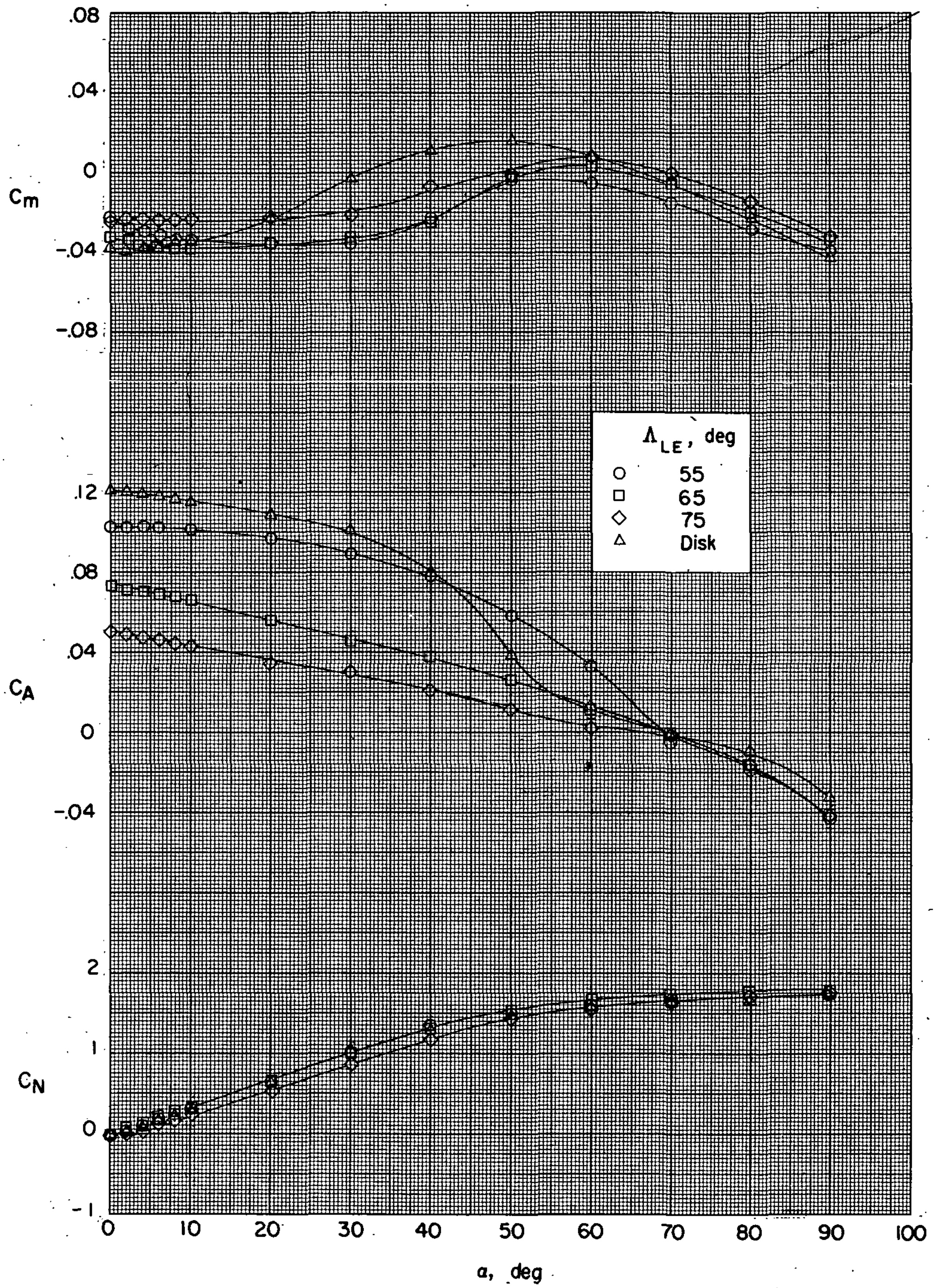


(a) $C_m$, $C_A$, and $C_N$.

Figure 5.- Aerodynamic characteristics of delta-wing models.

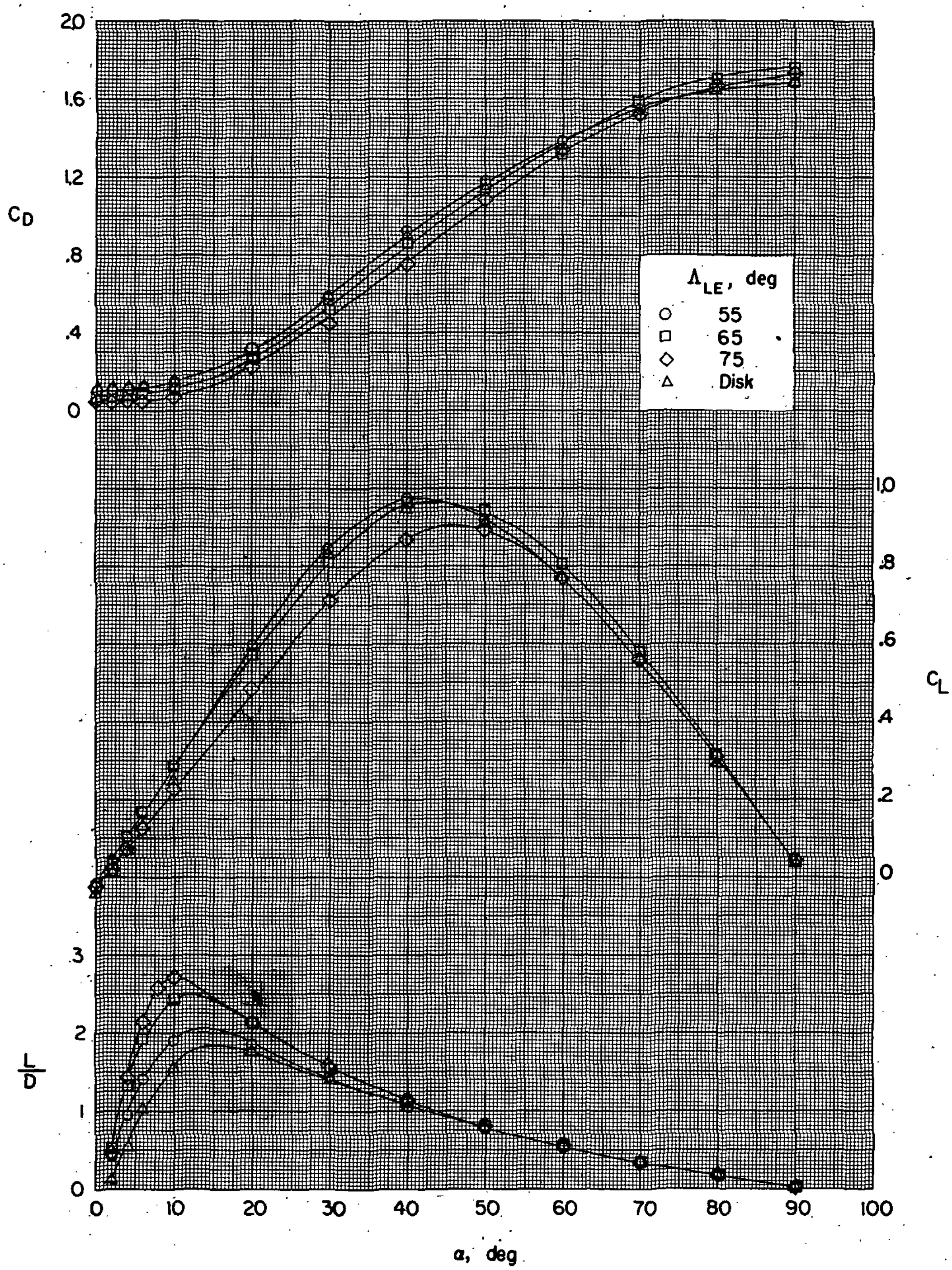


(b) $C_D$, $C_L$, and L/D.

Figure 5.- Concluded.

L-650

L-650

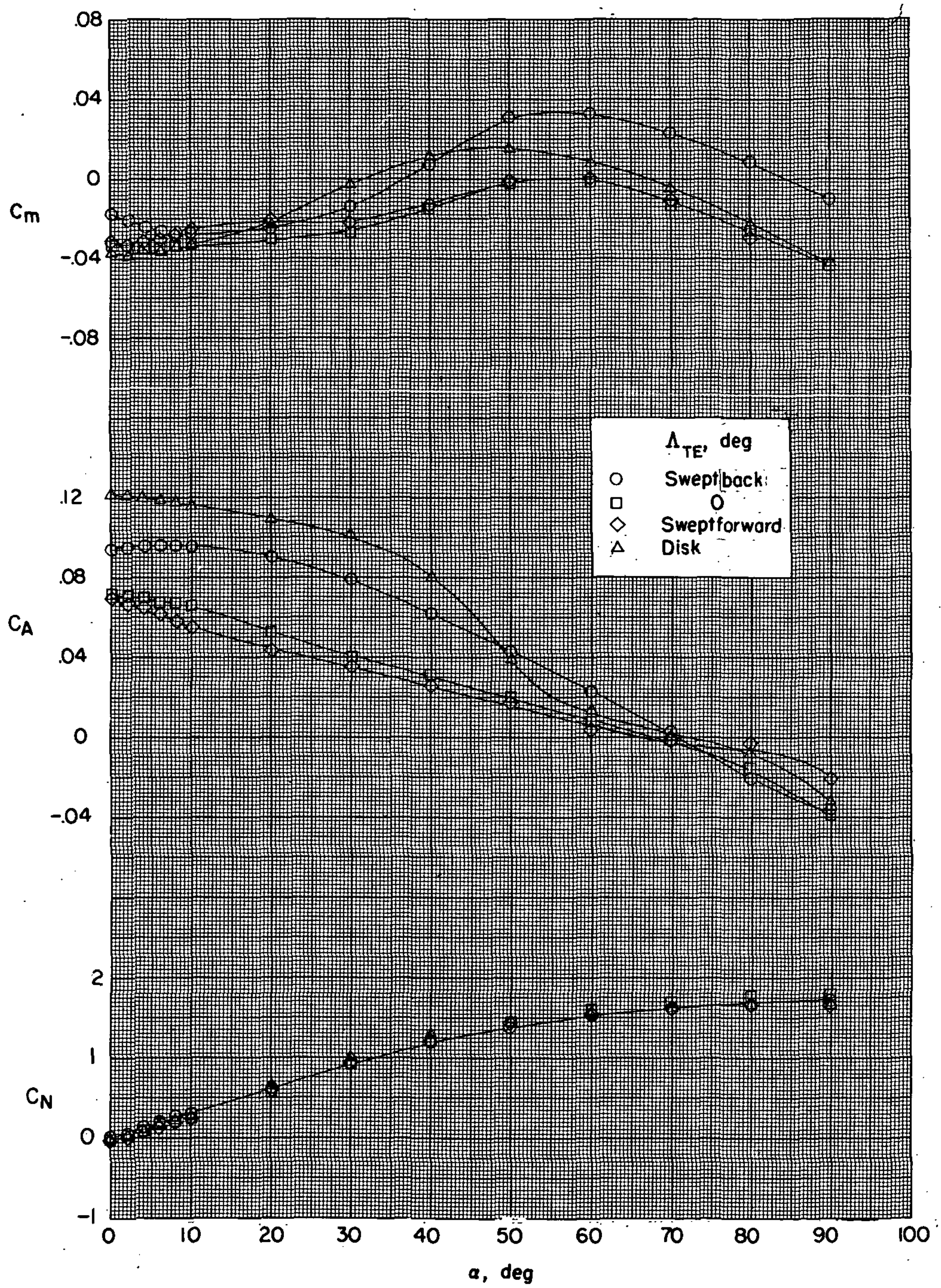


(a) $C_m$, $C_A$, and $C_N$.

Figure 6.- Aerodynamic characteristics of trailing-edge sweep models.

DECLASSIFIED



CONFIDENTIAL

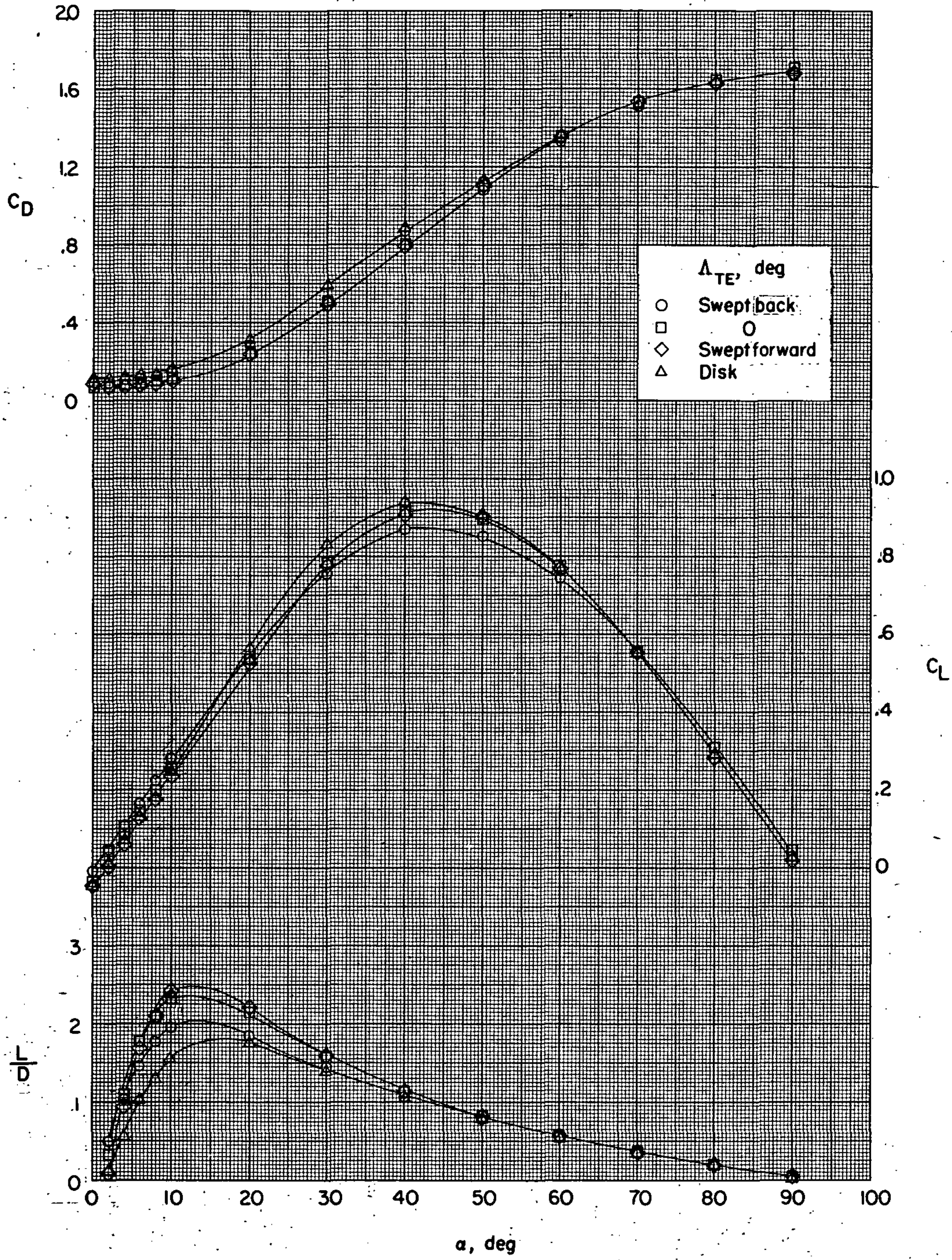


(b) $C_D$, $C_L$, and L/D.

Figure 6.- Concluded.



L-650

DECLASSIFIED